



CARITAS UNIVERSITY AMORJI-NIKE, EMENE, ENUGU STATE

Caritas Journal of Engineering Technology

CJET, Volume 3, Issue 2 (2024)

Article History: Received: 15th August, 2024 Revised: 27th September, 2024 Accepted: 20th October, 2024

Design of a Continuous Stirred Tank Reactor for Optimum Production of 1,000,000 tons per year of Ethylene Glycol

¹Oba, Israel

¹Akpa, Jackson Gunorubon

^{*2}Wosu, Chimene Omeke

¹Department of Chemical/Petrochemical Engineering, Rivers State University, Nigeria

²Department of Chemical Engineering, Federal University Otuoke, Bayelsa, Nigeria.

*Corresponding Author: wosuco@fuotuoike.edu.ng

ORCID: <https://orcid.org/0009-0007-1766-649X>

Abstract

The liquid phase hydrolysis reaction of ethylene oxide is most suitable in a Continuous Stirred Tank Reactor (CSTR) because of the nature of reactants or feed materials for ethylene glycol production. Based on the economic importance of ethylene glycol as an organic compound and chemical intermediate utilized domestically and industrially as a feedstock for the production of paint, plastic, printing inks, hydraulic fluids, reagents in making polyesters, explosives, synthetic waxes, automotive radiator coolants or antifreeze, etc. This research however becomes highly imperative as it considers or incorporates important objectives or steps for optimum production of ethylene glycol which are stated sequentially as follows. Firstly the design aspect of this research involves the development of CSTR performance or sizing models using the first principle of material and energy balance. The developed models were simulated using the advanced process simulation tool MATLAB R2023a version and the optimum values of reactor parameters like volume, height, diameter, space-time, space velocity, quantity of heat generated and quantity of heat per unit volume of the reactor are 11.160m³, 3.845m, 1.922m, 279.011sec, 0.004sec⁻¹, 2.507J/s and 0.225J/sm³ respectively. Secondly, the reactor production cost as a function of its volume in dollars and naira was estimated every year as 799.955 in dollars and 1,309,255.2 in naira as of 21st September 2024. Finally, the analysis of the design results showed that the continuous stirred tank reactor (CSTR) is most economically suitable for optimum production of ethylene glycol in industries.

Keywords: CSTR, Ethylene Glycol, Design Models, Petrochemicals.

1. INTRODUCTION

The continuous Stirred Tank Reactor (CSTR) is of great importance in the Chemical/Petrochemical Engineering field because of its capability of converting or transforming raw materials into finished products (Levenspiel, 1999). Based on the economic importance of chemical reactors, process industries and researchers in chemical and petrochemical engineering fields are faced with the task of properly studying the reactor, its operation, configurations, factors affecting it and how to effectively and efficiently utilize the principles of mass and energy balance to develop the reactor design models (Wordu & Wosu, 2019; Wosu *et al.*, 2024a).

Industrially, ethylene glycol can be produced from the oxidation of ethylene to form ethylene oxide which is hydrolyzed to produce ethylene glycol in a continuously stirred tank reactor (Wosu *et al.*, 2024b). The reactor choice depends on the nature of the reactant species (ethylene oxide and water) and the phase of the reaction. The petrochemical product (ethylene glycol) is regarded as the simplest diol or glycol, the first of a homologous series of three dihydroxy alcohols namely, mono ethylene glycol (MEG), diethylene glycol (DEG) and triethylene glycol (TEG). It is an important organic compound and chemical intermediate used in a large number of industrial processes such as paint production, plastics, solvents, coolants or antifreeze in automotive radiators, heat transfer fluids, raw material in the production of polyester, fibres for clothes, upholstery, carpet, pillows, printing inks, reagents in making polyesters, explosives, synthetic waxes and production of pet bottles (Wosu & Ezech, 2024)

Several types of research have been done on the design of continuous stirred tank reactors for the production of petrochemicals and thus;

Akpa & Onuora (2018) researched on Simulation and control of a reactor for the non-catalytic hydrolysis of ethylene oxide to ethylene glycol. According to the researchers, ethylene glycol, also called ethane-1,2-diol is an organic compound that is often used in the production of polyester, fibre fabrics, solvents for paints and plastics etc. Ethylene glycol (EG) production in industries can either be via a catalytic process where the reaction is catalyzed by an acid or base or non-catalytic where the reaction occurs at neutral PH and appreciable rise in temperatures. The latter is most widely used (Samoilov & Mnushkin, 2012)

The flow diagram for the non-catalytic hydrolysis of ethylene oxide for ethylene glycol production is shown in Figure 1.

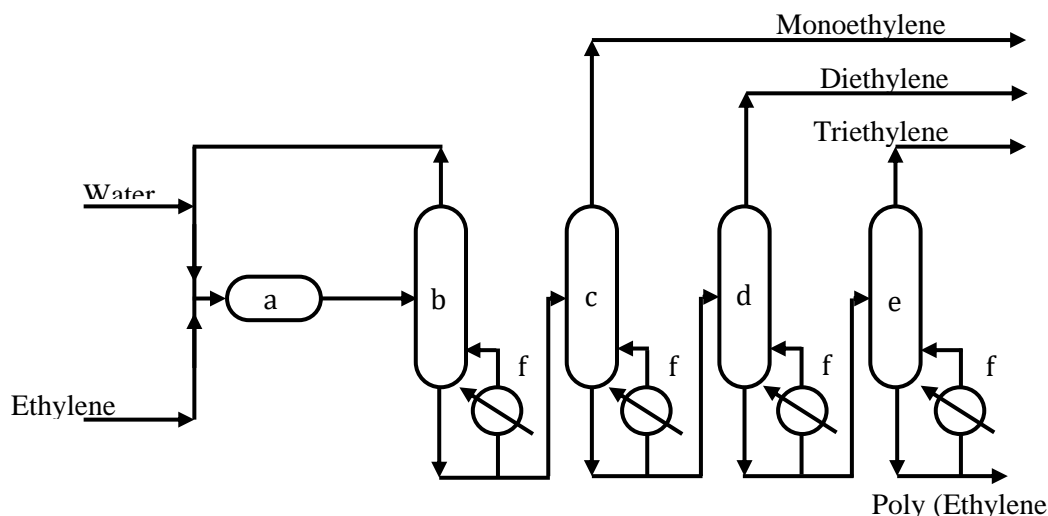


Figure 1: Hydrolysis of Ethylene Oxide (Arrieta, 2001).

**(a) Reactor (b) Evaporator (c) MEG column (d) DEG column (e) TEG column
(f) Reboilers**

Ethylene oxide stream is first contacted with water in a gas absorber at an ethylene oxide (EO) to water ratio of about 1:20. The formation of higher homologous is reduced by releasing the ethylene oxide solution to a temperature of about 200°C and fed to a continuous stirred tank reactor (CSTR) where it is thermally hydrolyzed to ethylene glycol at an operating temperature of about 190-200°C and pressure of about 14-22atm. Ethylene oxide reacts further with mono-ethylene glycol (MEG) and higher homologues in a series-parallel reaction to form di-ethylene and tri-ethylene glycol. Consequently, the water-ethylene glycol mixture from the reactor is transferred to the first stage of multi-stage evaporators where high-pressure steam is used to reboil the mixture thereby separating ethylene glycol to mono ethylene. For oxide-ethylene glycol reaction occur (Mellem, *et al.*, 2001). This proceeding which is usually a rapid or fast reaction in nature makes the control of the process highly imperative and necessary.

Higher glycols like di, tri, tetra etc. can be formed through this continuous addition polymerization reaction. The most important process variable affecting this production process is the quantity of water which should be in excess (almost 20 times greater than the ethylene oxide) (Rebsdatt & Mayor, 2005). For industrial applications in commercial plants, excess water is recommended for high selectivity and to achieve at least a 90% conversion of ethylene oxide to mono-ethylene glycol (MEG) (Arrieta, 2001). To maintain this condition of ethylene oxide-water ratio requirement, a high level of control mechanism must be in place. Hence, the researchers focused on applying the principles of material and energy balance to develop models that are capable of controlling the input, output as well as disturbances in the system and how they can be manipulated or controlled using appropriate closed loop models with proportionality. Integral-derivative controller capable of bringing the system back/close to its original set point value and ensuring stability of the process.

Batiha (2004a) Researched dynamic modelling of the non-catalytic process of ethylene oxide hydrolysis. According to the researcher, one of the most relevant processes of organic synthesis is the production of mono-ethylene glycol (MEG) also called ethylene glycol and its analogs: di-, tri-tetra-, and poly-ethylene glycols. This ethylene glycol is mostly used in the production of polyethylene terephthalate and antifreeze while di and tri-ethylene glycols are used in resin for the gas drying process (Landau & Ozero, 1982). Batiha included that ethylene glycol is produced generally from the hydrolysis of ethylene oxide in the absence of a catalyst.

Batiha (2004b) also researched on kinetic investigation of consecutive-parallel reactions in the non-catalytic process of ethylene oxide hydrolysis. The researcher also stated that consecutive parallel reactions can be used in the technology of organic synthesis such as the non-catalytic hydrolysis of ethylene oxide (EO) for the production of mono ethylene glycol (MEG) and other reactions products like di-, tri-, tetra-, and polyethylene glycols. The above process is described as the most widespread way of ethylene glycol synthesis because it is simple and economically efficient (Sherwood, 1959).

Wosu (2024) researched on design of CSTR for the production of magnesium chloride from the neutralization reaction of magnesium oxide and hydrochloric acid. According to the researcher, the design of process equipment (reactor) simply involves sizing of the equipment which involves determination of the reactor volume (V_R), height (H_R), diameter (D_R), space time (τ_{CSTR}), space velocity (S_V) etc.

Braide *et al.* (2021) researched the production of ethylene oxide in a packed column using the computer as the design tool. The researchers focused on the design of a packed column, plug flow reactor and distillation column for the production of ethylene oxide. The design models of the equipment were developed by application of the principle of mass and energy balance across the equipment. The effect of the reactor parameters such as volume, height and heat on the fractional conversion were shown in plots or profiles. This research, however, did not consider the development of the dynamic models of equipment as well as the control models but centred on equipment sizing.

2. Materials and Methods

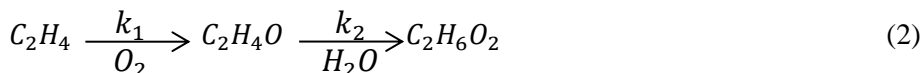
The materials utilized in this research are the calculated/derived data, data obtained from valid literature and process or design simulation software. The research methodology is quantitative and the steps adopted include;

2.1 Reaction Kinetic Scheme Development

The stoichiometry of the reaction process is utilized in the development of the reaction kinetic models of the process. The chemistry of the process involves the reaction of ethylene and oxygen to produce ethylene oxide which reacts further with water to produce ethylene glycol. The reaction between ethylene and oxygen is called an oxidation reaction while that of ethylene oxide with water is called a hydrolysis reaction. The combination of both reactions is called a series section as shown below:



Equation (1) can be expressed molecularly as



Symbolically, equation (2) can be expressed as:



Where A represents ethylene, B is ethylene oxide and C represents ethylene glycol, k_1 and k_2 represents the kinetic rate constants which is an indication that the reaction process is temperature-dependent and the process condition is non-isothermal. The rate constants are a function of temperature and activation energy as shown in equations (4) and (5) respectively.

$$k_1 = k_{10}e^{(-E_1/RT)} \quad (4)$$

$$k_2 = k_{20}e^{(-E_2/RT)} \quad (5)$$

Where k_{10} is the Arrhenius constant also called the pre-exponential constant of the first reaction process for the production of ethylene oxide from ethylene, k_{20} is also the Arrhenius or pre-exponential constant of the second reaction process for the production of ethylene glycol from the hydrolysis of ethylene oxide, E_1 and E_2 are the activation energies in kJ/kmol of ethylene oxide and ethylene glycol respectively. T_1 and T_2 are the respective temperatures of the processes in Kelvin and R is the gas constant in J/mol.k.

The rate expression of the series of reactions occurring consecutively can be expressed as a function of feed rate depletion as follows;

For the depletion of ethylene to produce ethylene oxide, the rate law can be expressed mathematically as:

$$-r_A = \frac{-dC_A}{dt} = k_1 C_A \quad (6)$$

Where $-r_A$ is the rate of depletion of ethylene, C_A Is the concentration of ethylene after the reaction in mol/m³ and t is the reaction time in seconds.

For the formation of ethylene oxide and its depleting rate for ethylene glycol production, the rate law can be expressed mathematically as;

$$-r_B = \frac{-dC_B}{dt} = -k_1 C_A + k_2 C_B \quad (7)$$

Finally, the rate law for the production of ethylene glycol from the depletion of ethylene oxide is mathematically expressed as:

$$-r_C = \frac{-dC_C}{dt} = -k_2 C_B \quad (8)$$

Where $-r_B$ is the rate of reaction for ethylene oxide formation and its depleting rate, $-r_C$ Is the ethylene glycol formation rate and C_B Is the concentration of ethylene oxide in mol/m³.

Substituting equations (4) and (5) into equations (6), (7) and (8) respectively yields

$$\frac{-dC_A}{dt} = k_{10}e^{(-E_1/RT_1)} C_A \quad (9)$$

$$\frac{-dC_B}{dt} = k_{20}e^{(-E_2/RT_2)} C_B - k_{10}e^{(-E_1/RT_1)} C_A \quad (10)$$

$$\frac{-dC_C}{dt} = k_{20}e^{(-E_2/RT_2)} C_B \quad (11)$$

Equation (11) is the rate expression or model for ethylene glycol production and can be expressed in terms of fractional conversion as follows:

$$-r_C = -k_{20} e^{-E_2/RT_2} C_{B0}(1 - X_B) \quad (12)$$

2.2 Development of the CSTR Design/Sizing Model

Consider the schematic representation of a continuously stirred tank reactor with feeds and products.

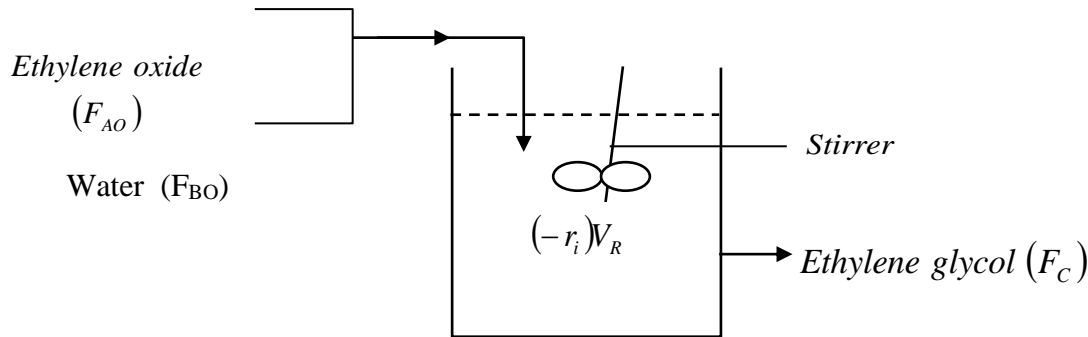


Figure 2: Continuous Stirred Tank Reactor

The feed stream consists of:

- i. Ethylene oxide
- ii. Water

While the product stream is Ethylene glycol

Assumptions

- i. The feed assumes a uniform composition throughout the reactor.
- ii. The reacting mixture is well stirred.
- iii. The composition of the exit stream is the same as that within the reactor.
- iv. Shaft work by the impeller or the stirrer is negligible.
- v. The temperature within the reactor is kept at a constant value by the heat exchange medium.

2.3 Volume of the Reactor Determination (V_R)

This can be obtained by applying the principle of material balance stated as follows:

$$\left[\begin{array}{c} \text{Rate of} \\ \text{Accumulation of} \\ \text{Product within} \\ \text{the Volume} \end{array} \right] = \left[\begin{array}{c} \text{Rate of Input} \\ \text{of Feed into} \\ \text{Volume} \end{array} \right] - \left[\begin{array}{c} \text{Rate of} \\ \text{Outflow of} \\ \text{Feed from} \\ \text{Volume} \end{array} \right] - \left[\begin{array}{c} \text{Rate of} \\ \text{Depletion of} \\ \text{Feed due to} \\ \text{Chemical} \\ \text{Reaction} \end{array} \right] \quad (13)$$

The terms in equation (13) can be defined as follows:

$$\left[\begin{array}{l} \text{Rate of} \\ \text{Accumulation of} \\ \text{Product within} \\ \text{the Volume} \end{array} \right] = \frac{d}{dt}(C_A V_R) \quad (14)$$

$$\left[\begin{array}{l} \text{Rate of Input of} \\ \text{Feed into Volume} \end{array} \right] = F_{AO} \quad (15)$$

$$\left[\begin{array}{l} \text{Rate of Output} \\ \text{of Feed from} \\ \text{Volume} \end{array} \right] = F_A = F_{AO}(1 - X_A) \quad (16)$$

$$\left[\begin{array}{l} \text{Rate of} \\ \text{Depletion of} \\ \text{Feed due to} \\ \text{Chemical} \end{array} \right] = (-r_A)V_R \quad (17)$$

Combining equation (14) to (17) into equation (13) yields

$$\frac{d}{dt}(C_A V_R) = F_{AO} - [F_{AO}(1 - X_A)] - (-r_A)V_R \quad (18)$$

At steady state, the accumulation term is equal to zero, i.e.

$$\begin{aligned} \frac{d}{dt}(C_A V_R) &= 0 \\ \therefore 0 &= F_{AO} - [F_{AO}(1 - X_A)] - (-r_A)V_R \end{aligned} \quad (19)$$

Expanding the bracket

$$0 = F_{AO} - F_{AO} + F_{AO}X_A - (-r_A)V_R$$

$$0 = F_{AO}X_A - (-r_A)V_R$$

$$V_R = \frac{F_{AO}X_A}{(-r_A)} \quad (20)$$

Substituting equation (12) into equation (20) yields

$$V_R = \frac{F_{AO} X_A}{A e^{-E/RT} C_{AO} (1 - X_A)} \quad (21)$$

2.4 Height of the Reactor Determination (H_R)

Since the reactor is cylindrical, the volume of a cylindrical reactor is given as

$$V_R = \pi R^2 L_R \quad (22)$$

where V_R is the volume of the reactor (m^3), R is the radius of the reactor (m), L_R is the height of the reactor (m) and π is Constant

Since the radius of a cylinder is half its diameter, that is;

$$R = \frac{D_R}{2} \quad (23)$$

where D_R is the diameter of the reactor (m).

Combining equation (22) and (23) yields

$$V_R = \pi \left(\frac{D_R}{2} \right)^2 L_R \quad (24)$$

For a CSTR, according to Perry et al., 2008,

$$\frac{L_R}{D_R} = 2 \quad (25)$$

$$D_R = \frac{L_R}{2} \quad (26)$$

Combining equation (26) and (24) yields

$$V_R = \frac{\pi \left(\frac{L_R}{2} \right)^2 L_R}{4}$$

$$V_R = \frac{\pi L_R^3}{16}$$

$$\therefore L_R = \left(\frac{16 V_R}{\pi} \right)^{1/3} \quad (27)$$

Substituting equation (21) into (27) yields

$$L_R = \left[\frac{16 F_{AO} X_A}{\pi A e^{-E/RT} C_{AO} (1 - X_A)} \right]^{1/3} \quad (28)$$

2.5 Diameter of the Reactor Determination (D_R)

From equation (26)

$$D_R = \frac{L_R}{2}$$

Substituting equation (28) into (26) yields

$$D_R = \frac{\left[\frac{16 F_{AO} X_A}{\pi \cdot A_e^{-E/RT} C_{AO} (1 - X_A)} \right]^{1/3}}{2} \quad (29)$$

2.6 Space-Time Determination (τ_{CSTR})

This is defined as the ratio of reactor volume and volumetric flow rate

$$\tau_{CSTR} = \frac{V_R}{v_O} \quad (30)$$

Substituting equation (21) into (30) yields

$$\tau_{CSTR} = \frac{\frac{F_{AO} X_A}{A_e^{-E/RT} C_{AO} (1 - X_A)}}{v_O} \quad (31)$$

$$F_{AO} = C_{AO} v_O \quad (32)$$

Substituting equation (24) into (31) yields

$$\tau_{CSTR} = \frac{X_A}{A_e^{-E/RT} (1 - X_A)} \quad (33)$$

2.7 Space Velocity Determination (S_V)

This is defined as the reciprocal of space time.

$$S_V = \frac{1}{\tau_{CSTR}} \quad (34)$$

Substituting equation (33) into (34) yields

$$S_V = \frac{A_e^{-E/RT} (1 - X_A)}{X_A} \quad (35)$$

2.8 Quantity of Heat Generated per unit Volume of the Reactor (q) and Energy Balance Model Development

The concept of heat (energy) balance in chemical reaction engineering is very important and is one of the basic factors affecting the rate at which a raw material (feed) is transformed into a finished product. In the production of ethylene glycol from the hydrolysis of ethylene oxide, the quantity of heat generated per unit volume of the reactor is defined as the ratio of the quantity of heat generated (Q) and the volume of the reactor (V_R).

This is mathematically given as,

$$q = \frac{Q}{V_R} \quad (36)$$

Where,

$$Q = \Delta H_R F_{AO} X_A \quad (37)$$

Therefore

$$q = \frac{\Delta H_R F_{AO} X_A}{V_R} \quad (38)$$

To account for the effect of temperature (heat) during the production of the petrochemical product (ethylene glycol), energy balance model development is an important tool. This model is governed by the principle of conservation of energy which can be stated mathematically as follows:

The Energy Balance for the Non-isothermal Continuous Stirred Tank reactor (CSTR) can be obtained using the general principle of conservation of material which is given as:

$$\left[\begin{array}{c} \text{Rate of} \\ \text{Accumulation of} \\ \text{Heat within the} \\ \text{Volume} \end{array} \right] = \left[\begin{array}{c} \text{Rate of Input} \\ \text{of Heat into} \\ \text{Volume} \end{array} \right] - \left[\begin{array}{c} \text{Rate of} \\ \text{Outflow of} \\ \text{Heat from} \\ \text{Volume} \end{array} \right] - \left[\begin{array}{c} \text{Rate of} \\ \text{Depletion of} \\ \text{Heat due to} \\ \text{Chemical} \\ \text{Reaction} \end{array} \right] \quad (39)$$

$$\left[\begin{array}{c} \text{Rate of Heat} \\ \text{Removal to the} \\ \text{Surrounding} \end{array} \right] \left[\begin{array}{c} \text{Shaft work} \\ \text{done by the} \\ \text{Stirrer} \end{array} \right]$$

The terms in equation (39) can be defined as follows:

$$\left[\begin{array}{c} \text{Rate of} \\ \text{Accumulation} \\ \text{of Heat within} \\ \text{the Volume} \end{array} \right] = \frac{d(\rho V C_p T)}{d\tau} \quad (40)$$

$$\left[\begin{array}{l} \text{Rate of Input} \\ \text{of Heat into} \\ \text{Volume} \end{array} \right] = \rho V_o C_p T_o \quad (41)$$

$$\left[\begin{array}{l} \text{Rate of} \\ \text{Outflow of} \\ \text{Heat from} \\ \text{Volume} \end{array} \right] = \rho V C_p T \quad (42)$$

$$\left[\begin{array}{l} \text{Rate of Depletion} \\ \text{of Heat due to} \\ \text{Chemical} \\ \text{Reaction} \end{array} \right] = (-r_A) V_R (\Delta H_R) \quad (43)$$

$$\left[\begin{array}{l} \text{Rate of Heat} \\ \text{Removal to the} \\ \text{Surrounding} \end{array} \right] = U A_C (T - T_C) \quad (44)$$

$$\left[\begin{array}{l} \text{Shaft work} \\ \text{done by the} \\ \text{Stirrer} \end{array} \right] = W_s \quad (45)$$

Combining equation (3.40) to (3.45) into equation (3.39) yields

$$\rho V_o C_p \frac{dT}{d\tau} = \rho V_o C_p T_o - \rho V_o C_p T - (-r_A) V_R (\Delta H_R) - U A_C (T - T_C) + W_s \quad (46)$$

Assumptions

- i. Constant density
- ii. The system operates at a steady state
- iii. Work done by the stirrer is negligible

At a steady state,

$$\frac{dH}{d\tau} = \rho C_p V \frac{dT}{dt} = 0$$

Also Neglecting the Shaft Work W_s

Equation (46) becomes

$$0 = \rho V_o C_p T_o - \rho V_o C_p T - (-r_A) V_R (\Delta H_R) - UA_C (T - T_C)$$

By rearranging and factorization

$$\rho V_o C_p (T - T_o) = - (-r_A) V_R (\Delta H_R) - UA_C (T - T_C)$$

Dividing through by $\rho V_o C_p$

$$T - T_o = - \frac{(-r_A) V_R (\Delta H_R)}{\rho v_o C_p} - \frac{UA_C (T - T_C)}{\rho v_o C_p} \quad (47)$$

But $\frac{V_R}{v_o} = \tau$ (space time)

$$T - T_o = \tau \frac{-\Delta H_R r_A}{\rho C_p} - \frac{UA_C (T - T_C)}{\rho v_o C_p} \quad (48)$$

Equation (48) can be rearranged to give

$$T = \frac{\tau \Delta H_R r_A V_o + UA_C T_C + \rho V_o C_p T_o}{\rho V_o C_p + UA_C} \quad (49)$$

2.9 Reactor Operating Parameters

The calculated/derived data and data obtained from valid literature for the design model simulation are presented in Table 1 below:

Table 1: Data Obtained from Literature

| Data | Values | Description | References |
|--------------|--|---|----------------------|
| T_o | 463k | The initial temperature of the feed | Akpa & Onuora (2018) |
| T | 473k | The operating temperature of the reactor | Akpa & Onuora (2018) |
| T_C | 468k | Coolant temperature | Akpa & Onuora (2018) |
| A_1 | $0.0442S^{-1}$ | Pre-exponential factor | Akpa & Onuora (2018) |
| A_2 | $0.0698S^{-1}$ | Pre-exponential factor | Akpa & Onuora (2018) |
| E_1 | 21193 kJ/mol | Activation energy | Akpa & Onuora (2018) |
| E_2 | 88.692 kJ/mol | Activation energy | Akpa & Onuora (2018) |
| K_1 | $7.2330S^{-1}$ | Rate constant | Akpa & Onuora (2018) |
| K_2 | $0.07143S^{-1}$ | Rate constant | Akpa & Onuora (2018) |
| ΔH_R | 2145.28 kJ/mol | Change in enthalpy of reactants. | Batiha (2004) |
| ΔC_p | 11664 kJ/°C | Change in specific heat capacity of reactants | Batiha (2004) |
| UA_C | 1.7 kg/m ² S ⁰ C | Heat transfer coefficient | Batiha (2004) |
| V_o | 0.041m ³ /s | Initial volumetric flow rate of reactants | Wosu et al, 2024b |

| | | | |
|----------|-------------------------|---|-------------------|
| C_{AO} | 0.030mol/m ³ | Initial concentration of ethylene oxide | Wosu et al, 2024b |
| F_{AO} | 0.00123mol/s | The initial molar flow rate of ethylene oxide | Wosu et al, 2024b |
| X_A | 0.95 | Maximum fractional conversion | Assumed |

2.10 Solution Techniques

The developed mass and energy balance models of the reactor were solved for the determination of the reactor design specification as well as other functional parameters using the advanced process simulation tool MATLAB R2023a version. The simulation process flow diagram is shown in Figure 3 below:

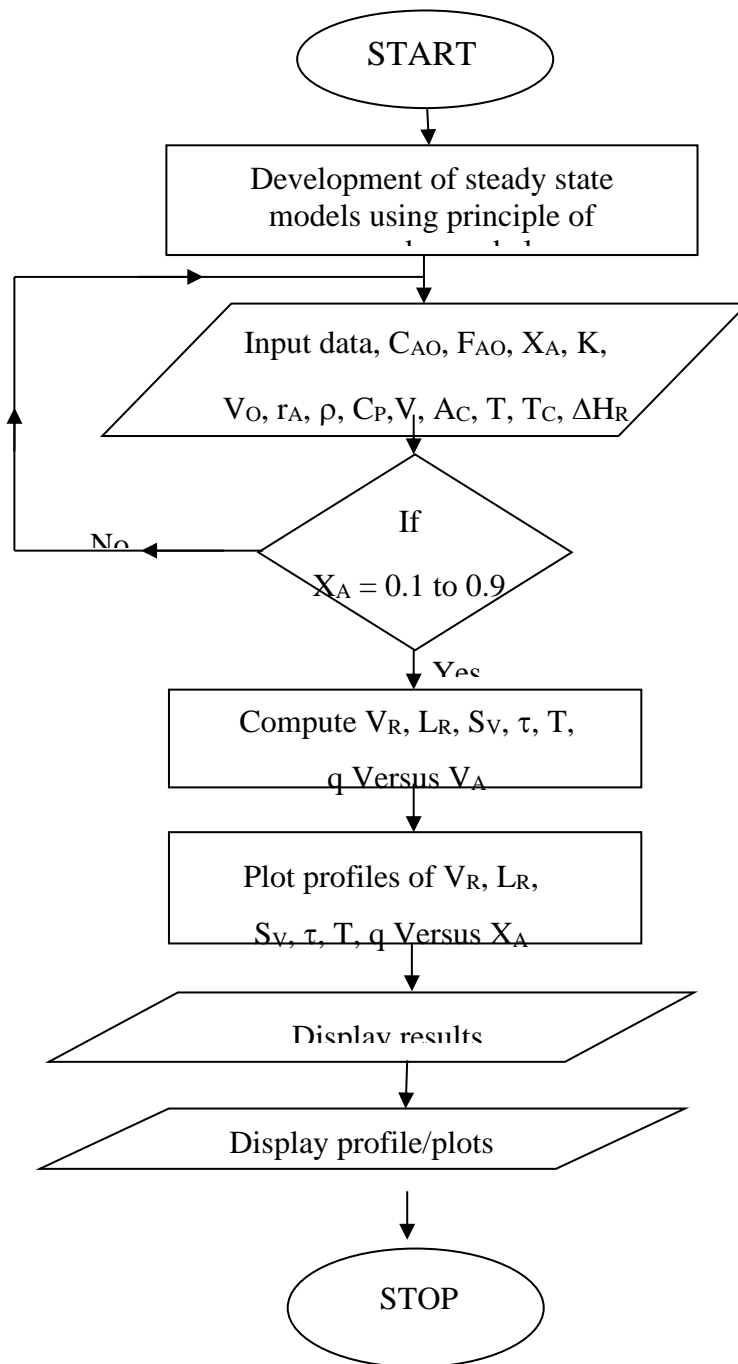


Figure 3: Simulation Process Flow Diagram

3 Results and Discussion

3.1 Design Results of Continuous Stirred Tank Reactor

The results of the continuous stirred tank reactor (CSTR) design for the production of 1 million tonnes (1,000,000,000kg) per year of ethylene glycol production at 95% fractional conversion is presented in Table 4.1 below:

Table 2: MATLAB Simulation Design Results Showing Fractional Conversion, Temperature, Volume of Reactor, Length of Reactor, Diameter of Reactor, Space-Time, Space Velocity, Quantity of Heat and Quantity of Heat per Unit Volume of the Reactor is Presented.

| X_A | T(K) | $V_R(m^3)$ | $L_R(m)$ | $D_R(m)$ | $\tau_{CSTR}(s)$ | $S_V(/S)$ | $Q(j/s)$ | $q(j/sm^3)$ |
|-------|---------|------------|----------|----------|------------------|-----------|----------|-------------|
| 0.000 | 463.000 | 0.000 | 0.000 | 0.000 | 0.000 | $Ln f$ | 0.000 | NaN |
| 0.050 | 466.299 | 0.031 | 0.540 | 0.270 | 0.773 | 1.294 | 0.132 | 4.268 |
| 0.100 | 469.597 | 0.065 | 0.693 | 0.346 | 1.632 | 0.613 | 0.264 | 4.043 |
| 0.150 | 472.895 | 0.104 | 0.808 | 0.404 | 2.591 | 0.386 | 0.396 | 3.818 |
| 0.200 | 476.194 | 0.147 | 0.908 | 0.454 | 3.671 | 0.272 | 0.528 | 3.594 |
| 0.250 | 479.492 | 0.196 | 0.999 | 0.500 | 4.895 | 0.204 | 0.660 | 3.369 |
| 0.300 | 482.791 | 0.252 | 1.086 | 0.543 | 6.293 | 0.159 | 0.792 | 3.145 |
| 0.350 | 486.089 | 0.316 | 1.172 | 0.586 | 2.907 | 0.126 | 0.924 | 2.920 |
| 0.400 | 489.387 | 0.392 | 1.259 | 0.629 | 9.790 | 0.102 | 1.055 | 2.695 |
| 0.450 | 492.686 | 0.481 | 1.348 | 0.674 | 12.015 | 0.083 | 1.187 | 2.971 |
| 0.500 | 495.984 | 0.587 | 1.441 | 0.720 | 14.685 | 0.068 | 1.319 | 2.246 |
| 0.550 | 499.282 | 0.718 | 1.541 | 0.770 | 17.948 | 0.056 | 1.451 | 2.021 |
| 0.600 | 502.581 | 0.881 | 1.649 | 0.825 | 22.027 | 0.045 | 1.583 | 1.797 |
| 0.650 | 505.897 | 1.091 | 1.771 | 0.886 | 27.272 | 0.037 | 1.715 | 1.572 |
| 0.700 | 509.177 | 1.371 | 1.911 | 0.956 | 34.265 | 0.029 | 1.847 | 1.348 |
| 0.750 | 512.476 | 1.762 | 2.078 | 1.039 | 44.054 | 0.023 | 1.979 | 1.123 |
| 0.800 | 515.774 | 2.350 | 2.287 | 1.144 | 58.739 | 0.017 | 2.111 | 0.898 |
| 0.850 | 519.073 | 3.329 | 2.569 | 1.284 | 83.214 | 0.012 | 2.243 | 0.674 |
| 0.900 | 522.371 | 5.287 | 2.997 | 1.499 | 132.163 | 0.008 | 2.375 | 0.449 |
| 0.950 | 525.669 | 11.160 | 3.845 | 1.922 | 279.011 | 0.004 | 2.507 | 0.225 |

Table 2: is a summary of the continuous stirred tank reactor design or sizing specification obtained from the MATLAB simulation of the CSTR design and energy balance model at various fractional conversion and operating temperatures. The results clearly showed that an increase in fractional conversion (X_A) and

temperature (T) increases the reactor volume (V_R), height (H_R), diameter (D_R), space-time (τ), and quantity of heat (Q) increases while the space velocity (S_V) and quantity of heat generated per unit volume of the reactor (q) decreases correspondingly. At a maximum fractional conversion of 0.95 and operating temperature of 525.669K, the reactor volume, height, diameter, space-time, space velocity, the quantity of heat generated and the quantity of heat generated per unit volume of the reactor were 11.160m³, 3.845m, 1.922m, 279.011sec., 0.004sec.⁻¹, 2.507J/s and 0.225J/sm³ respectively.

3.2 Results of Continuous Stirred Tank Reactor Functional Parameters Relationship

The effect of fractional conversion on reactor parameters and the relationship between reactor parameters were studied and displayed in the profiles below.

3.2.1 Variation of Reactor Volume (V_R) with Fractional Conversion (X_A)

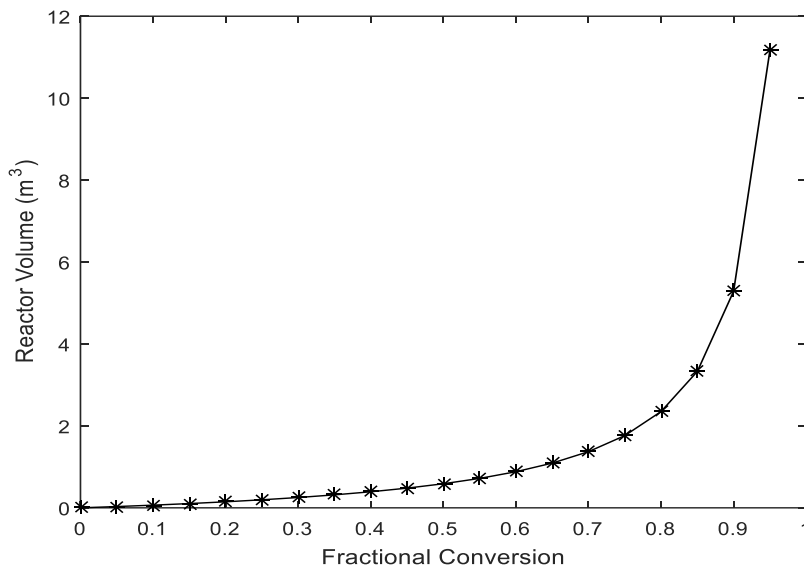


Figure 4: Plots of Reactor Volume (V_R) with Fractional Conversion (X_A)

Figure 4: represents the variation or relationship between the reactor's volume (m³) and fractional conversion.

From the graph above, the reactor volume varies exponentially with the fractional conversion i.e.

$$V_R \propto e^{X_A} \quad (50)$$

Introducing a constant of proportionality k, equation (50) transforms to

$$V_R = ke^{X_A} \quad (51)$$

Where V is the dependent variable, X_A Is the independent variable and k is the constant of proportionality and takes values from $0 < k < 5$ for instance,

When $X_A = 0.1, k < 1$ and when $X_A = 0.9, k < 3$

This implies that the best volume suitable for the process lies between $0.7 < e^{X_A} < 0.95$ and higher fractional conversion values say $X_A = 0.95$ will give a very high volume of the reactor and approaches positive infinity. This will make it impossible for the system to operate effectively, economically and optimally. Hence, the optimum volume occurs at $V = 11.16\text{m}^3$ and $X_A = 0.95$ as shown in the profile.

3.2.2 Variation of Reactor Height (H_R) with Fractional Conversion (X_A)

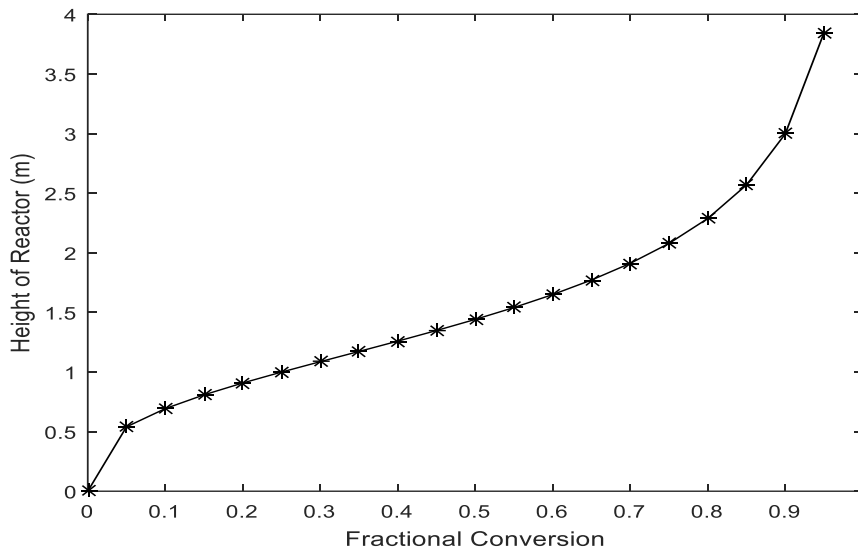


Figure 5: Plot of Reactor Height (H_R) with Fractional Conversion (X_A)

Figure 5 shows the variation or relationship between reactor height (m) and fractional conversion. The graph above depicts a progressive increase in reactor height as the fractional conversion increases. Initially, a linear increase in reactor height is exhibited from $H_R = 0$ to $H_R = 0.5$ at fractional conversion between $X_A = 0$ to $X_A = 0.05$. That is,

$$H_R \propto X_A \quad (52)$$

Then, the increment in height becomes exponential at fractional conversion (X_A) between 0.05 to 0.95 that is,

$$H_R \propto e^{X_A} \quad (53)$$

Combining equation (52) and (53) yields

$$H_R \propto X_A e^{X_A} \quad (54)$$

$$H_R = k X_A e^{X_A} \quad (55)$$

Equation (55) shows that reactor height varies directly as fractional conversion and also varies exponentially as fractional conversion. This shows that a fractional conversion (X_A) of 0.95, gives an optimum value of reactor height $H_R = 3.845m$.

Thus, the best range of fractional conversion X_A is $0.5 < X_A < 0.95$ which gives an optimum reactor height within the range of $1.3m < H < 3.845m$.

3.2.3 Variation of Reactor Diameter (D_R) with Fractional Conversion (X_A)

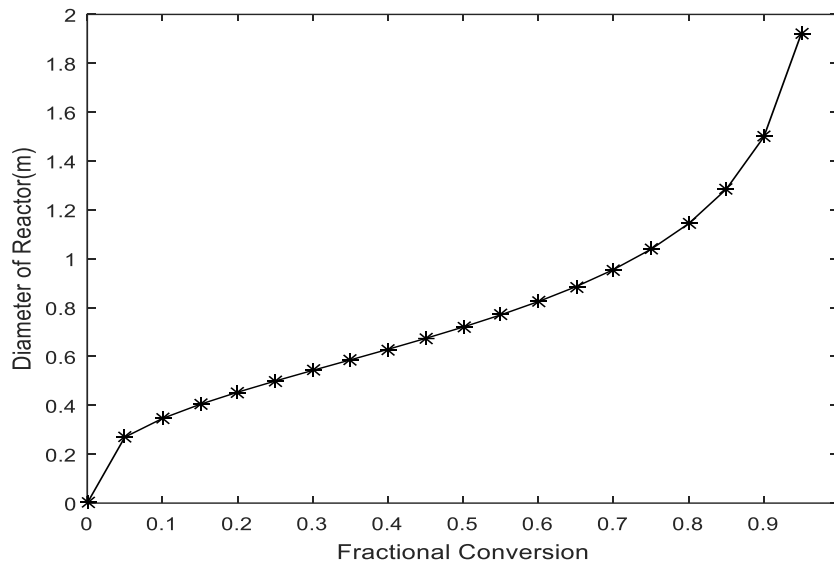


Figure 6: Plot of Reactor Diameter (D_R) with Fractional Conversion (X_A)

Figure 6 shows that the relationship between reactor diameter (D_R) and fractional conversion (X_A) is similar to that of the reactor height (H_R) and fractional conversion. Here, a linear increase of reactor diameter is exhibited from $D_R = 0.3$ at fractional conversion (X_A) between 0 to 0.05, thereafter an exponential increase in reactor diameter is shown at $X_A = 0.95$. This shows that at fractional conversion $X_A = 0.95$ gives an optimum value of reactor diameter $D_R = 1.922m$. Hence, the best or suitable range of reactor operation and optimal production is when the fractional conversion value lies within $0.5 < X_A < 0.95$ and $0.720m < D_R < 1.922m$.

3.2.4 Variation of Space-Time (τ_{CSTR}) with Fractional Conversion (X_A)

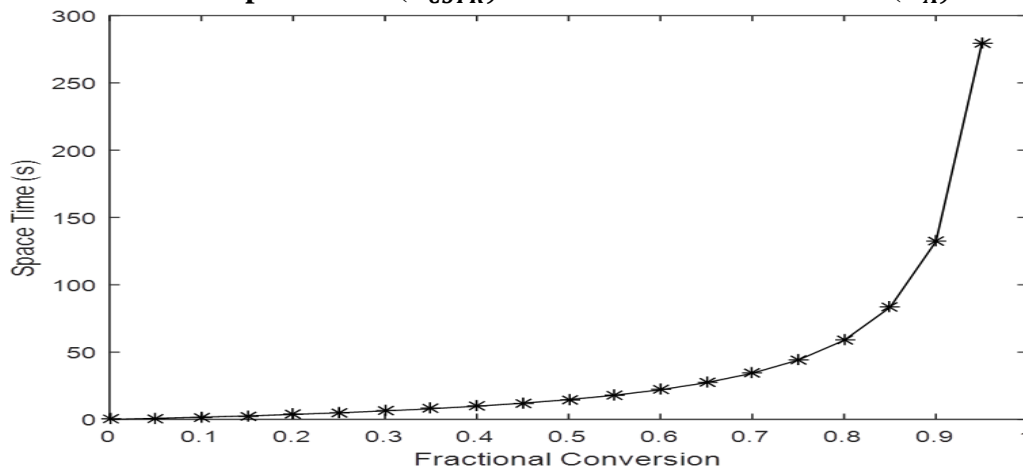


Figure 7: Plot of Space-Time (τ_{CSTR}) with Fractional Conversion (X_A)

Figure 7 shows a variation profile of space-time τ (S) and fractional conversion. X_A . Here, it is observed that the space-time (τ_{CSTR}) increases exponentially with the fractional conversion X_A . Depending on the proportionality constant. From $X_A = 0$ to $X_A = 0.75$, τ_{CSTR} increases exponentially from $\tau_{CSTR} = 0\text{sec}$ to $\tau_{CSTR} = 50\text{sec}$. Higher values of fractional conversion increase τ_{CSTR} to infinitesimal values. Hence, optimal space-time τ_{CSTR} occurs when fractional conversion $X_A = 0.8$. This ensures the optimal operation of the continuously stirred tank reactor.

3.2.5 Variation of Space Velocity (S_V) with Fractional Conversion (X_A)

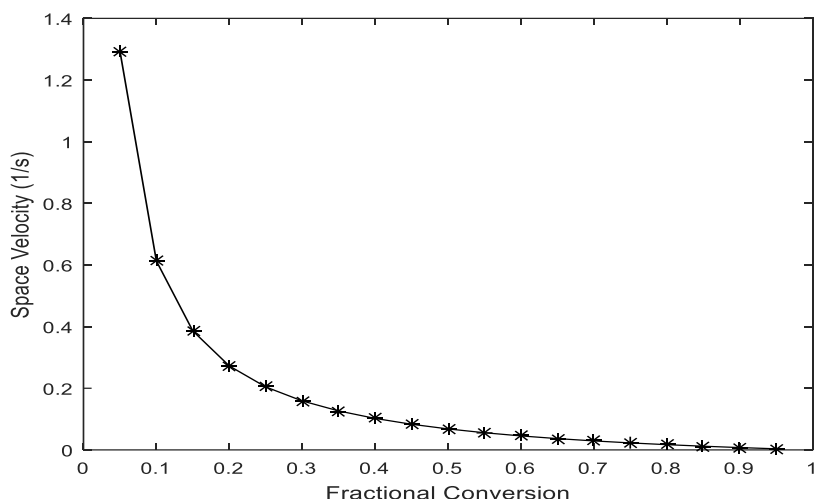


Figure 8: Plot of Space Velocity (S_V) with Fractional Conversion (X_A)

The profile trend in Figure 8 depicts the variation or changes between space velocity (S_V) and fractional conversion X_A . The relationship exhibits inverse exponential characteristics which can be expressed mathematically as,

$$S_V \propto e^{-X_A} \quad (56)$$

Smaller values of X_A Between 0 to 0.099 gives large values of S_V but as fractional conversion X_A increases from 0.1 to 0.95, the space velocity (S_V) decreases exponentially from $S_V = 0.614s^{-1}$ to $S_V = 0.004s^{-1}$. This clearly shows that the optimal condition of the CSTR occurs within the fractional conversion range of $0.45 < X_A < 0.9$.

7.2.6 Variation of Quantity of Heat (Q) with Fractional Conversion (X_A)

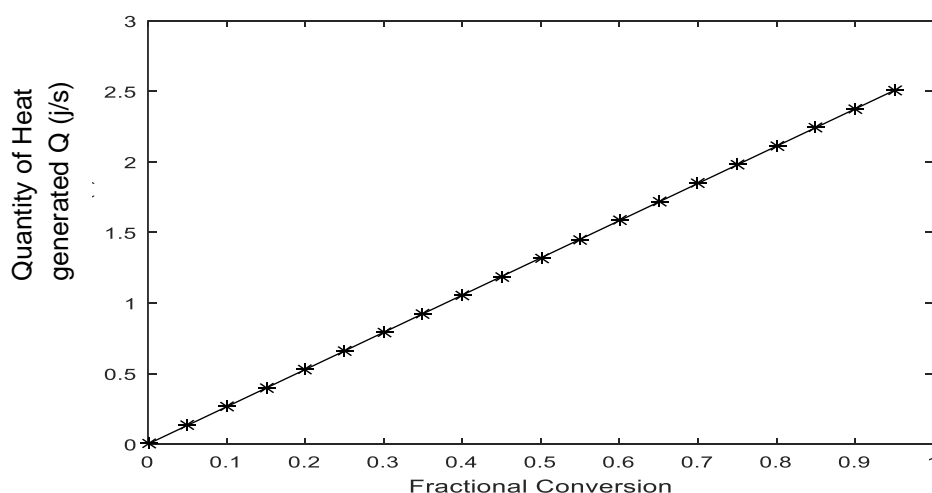


Figure 9: Plot of Quantity of Heat with Fractional Conversion (X_A)

Figure 9 above shows the quantity of heat (Q) profile with fractional conversion (X_A). The quantity of heat generated in the reactor varies directly proportional to the fractional conversion and can be expressed mathematically as,

$$Q \propto X_A \quad (57)$$

Introducing a constant of proportionality k

$$Q = kX_A \quad (58)$$

At X_A between 0.1 to 0.95, $k < 3$ and the optimum quantity of heat $Q = 2.507\text{J/s}$ is obtained at $X_A = 0.95$.

3.2.7 Variation of Quantity of Heat Generated per Unit Volume of Reactor (q) with Fractional Conversion (X_A)

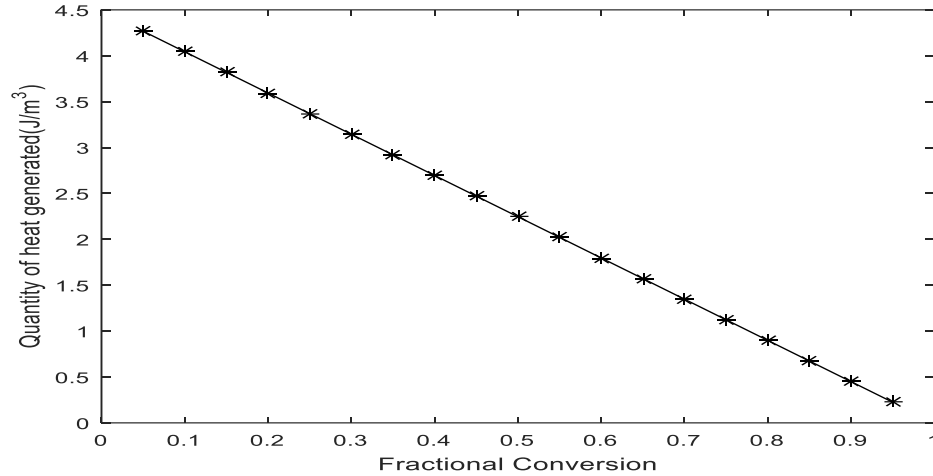


Figure 10: Plot of Quantity of Heat Generated per Unit Volume of Reactor (q) with Fractional Conversion (X_A)

The profile of the quantity of heat generated per unit volume of the reactor with fractional conversion exhibits an inverse variation relationship which can be expressed mathematically as,

$$Q \propto 1/X_A \quad (59)$$

$$Q = k/X_A \quad (60)$$

Lower values of fractional conversion, say $X_A = 0$ to 0.1 gives higher values of the quantity of heat generated per unit volume of the reactor. Hence, the optimal value of the quantity of heat generated per unit volume of the reactor is obtained at 0.95 fractional conversion, that is, $q_{\text{optimum}} = 0.225\text{J/Sm}^3$

3.2.8 Variation of Temperature (T) with Fractional Conversion (X_A)

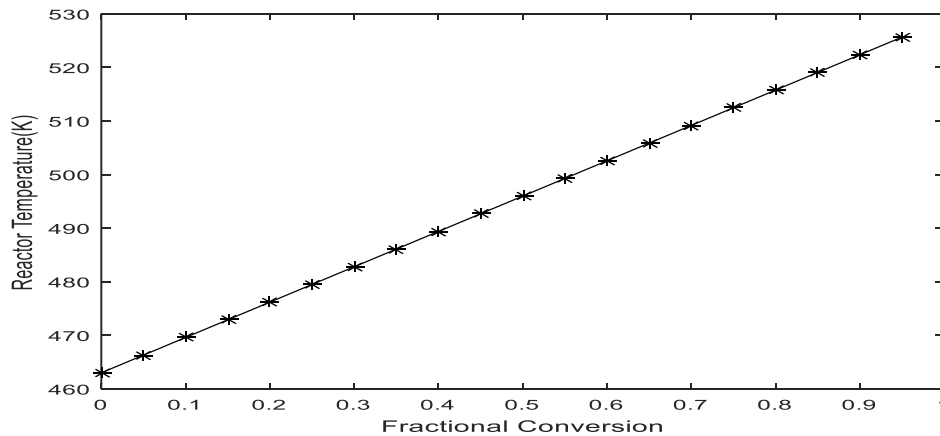


Figure 11: Plot of Temperature with Fractional Conversion

Figure 11 shows there is a direct proportionality variation between the temperature (T) and fractional conversion. X_A Which can be stated mathematically as,

$$T \propto X_A \quad (61)$$

Introducing a constant of proportionality k, equation (61) transforms to

$$T = kX_A \quad (62)$$

This shows that the reaction is endothermic and very little amount of heat is needed for a reaction to proceed. The graph also shows that the temperature needed for a reaction to proceed is 463k and a very negligible amount of heat is further added for the reaction process to achieve optimum yield.

3.2.9 Variation of Space-Time (τ_{CSTR}) with Volume of Reactor (V_R)

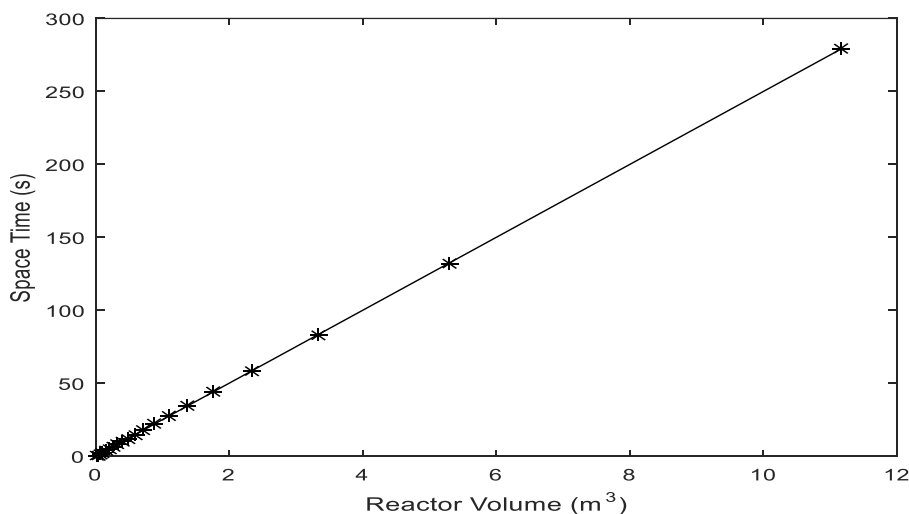


Figure 12: Plot of Space-Time with Reactor Volume

Figure 12 typically represents the relationship between space-time and reactor volume. The profile shows a linear correlation which can be stated mathematically as,

$$\tau_{CSTR} \propto V_R \quad (63)$$

The relationship in equation (63) shows that the space-time increases correspondingly with reactor volume and the optimal space-time values are concentrated between 0 to 90sec at a reactor volume between 0 to $3.5m^3$.

3.2.10 Variation of Space Velocity (S_V) with Volume of Reactor (V_R)

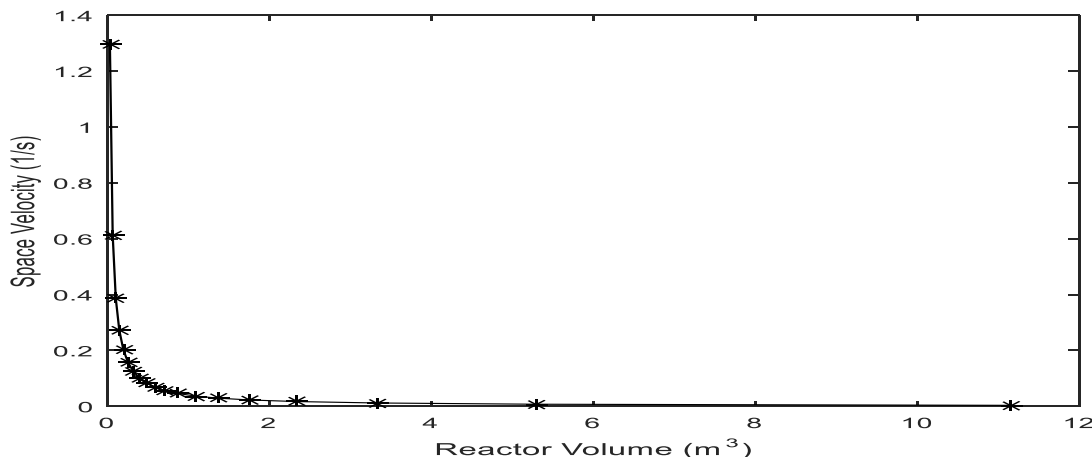


Figure 13: Plot of Space Velocity with Reactor Volume

Figure 13 depicts a profile of space velocity (S_V) and reactor volume (V_R) which clearly shows an exponential relationship where the maximum space velocity of $1.294s^{-1}$ occurs when the reactor volume V_R is $0m^3$. Also, when the space velocity exponentially drops to $S_V = 0.5^{-1}$ a higher volume of the reactor is obtained. Hence, the optimal yield of reactor volume $V_R = 11.16m^3$ is obtained at lower values of space velocity (S_V).

3.2.11 Variation of Reactor Volume (V_R) with Temperature (T)

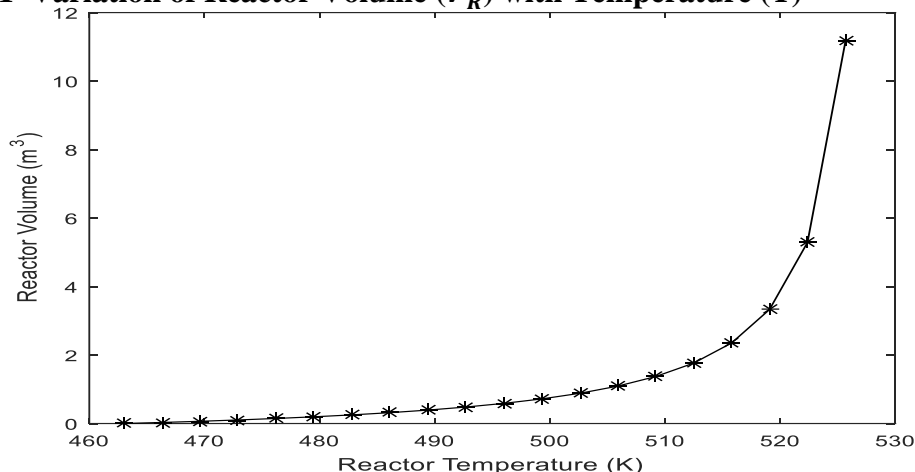


Figure 14: Plot of Reactor Volume with Temperature

Figure 14 above represents the profile or relationship between the reactor volume (V_R) and the temperature (T). Here, the reactor volume varies exponentially with the temperature of the reactor and can be represented mathematically as,

$$V \propto e^T \quad (64)$$

When the volume of the reactor is $0m^3$, the temperature of the reactor increases. The volume increases exponentially at temperature $T = 463 k$, and a large volume of the reactor is obtained and approaches positive infinity $V = +\infty$. Hence, optimum volume is obtained at a temperature range of $464 k < T < 520k$.

Conclusion

This research presents a comprehensive investigation of the continuously stirred tank reactor design for ethylene glycol production from a series of reactions involving the oxidation of ethylene to ethylene oxide and hydrolysis of ethylene oxide to produce ethylene glycol. The CSTR design model was developed from the conservation law of materials and was simulated using MATLAB R2023a version at various fractional conversions. The optimum specification of the reactor volume, height, diameter, space-time, space velocity, quantity of heat generated and quantity of heat generated per unit volume of the reactor were obtained as $11.160m^3$, $3.845m$, $1.922m$, $279.011sec.$, $0.004sec^{-1}$, $2.507J/s$ and $0.225J/m^3s$ at fractional conversion of 95%. The yearly production cost of ethylene glycol dependent on the reactor volume was given as 799.955 in dollars and 1,309,255.2 in naira respectively. The research demonstrates the feasibility of ethylene oxide hydrolysis in a CSTR for efficient ethylene glycol production, vital for domestic and industrial applications.

REFERENCES

- Akpa, J. G. & Onuorah, P. (2018). Simulation and control of reactor for the non-catalytic hydrolysis of ethylene oxide to ethylene glycol. ISSN 2224-5804 (Paper) ISSN 2225-0522 (Online), 8 (2).
- Arrieta, J. (2001). Ethylene glycol retrieve from [http://nataha.eng.usf.edu/gilbert/coused/model and analysis/portfolio](http://nataha.eng.usf.edu/gilbert/coused/model%20and%20analysis/portfolio).
- Batiha, M.M. (2004a). Dynamic modeling of the non-catalytic process of ethylene oxide hydrolysis. *Journal of Science & Technology* vol.(9) (1&2), 17-27.

- Batiha, M.M. (2004b). Kinetic investigation of connective parallel reaction in the non-catalytic process of ethylene oxide hydrolysis. *Journal of King Abdulaziz University. Engineering Science* vol. 15, (1), 19-31.
- Braide, D.T., Goodhead, T.O., Ademiluyi, F.T. & Ukpaka, C.P. (2021). Computer aided design of a packed bed reactor for the production of ethylene oxide. *Journal of Science and Engineering Research*, 8(2): 121-139, ISSN: 2394-2630. Available online www.jsaer.com
- Landau, R. & Ozero, B..J. (1982). Ethylene Glycol, Encyclopedia of Chemical Processing and Design, 2-52.
- Levenspiel, C. (1999). Chemical Reaction Engineering, (3rd Edition). John Wiley & Son's INC, USA.
- Mellem, S. A., Gianetto. A., Levin, M.E. Fisher, H.G., Chipett., S., Singh, S.K. & Chipman, P.L (2001) kinetics of the reactions of ethylene oxide with water and ethylene glycols, process safety progress, 20, 4, 231-246.
- Miki, M., Jto, J. & Ouchital, H. (1966). Reaction of ethylene oxide with active hydrogen., *Journal of Japan Oil Chemical Society*, 15(1); 257-26.
- Rebsdat S. & Mayer, D (2005). Ethylene oxide in: Ulmann's Encyclopedia of Industrial Chemistry, 7th e.d., Wienlein, Wiley-VCH publishers (online).
- Samoilov N.A & Mushkin, I. A. (2012). Mathematic modeling pronation stage of reactive distillation process for production of ethylene glycol. *Electronic Scientific Journal "oil and gas business"* 4 158-154.
- Shargarodski, M. A., Gordeev, L. S., Groshev, G.L. & Labutin, A.N. (1986). Kinetics of the non-catalytic reaction of ethylene oxide. *Russian Journal of Chemistry and Technology*, 29(10), 136-139.
- Sherwood H (1959). Three methods of ethylene glycol synthesis, ind. Chemist 35 (409) 126-131.
- Wordu, A.A. & Wosu, C.O. (2019). CSTR design for propylene glycol chemical production. *International Journal of Latest Technology in Engineering, Management & Applied Science (IJLTEMAS)*, 8(2), ISSN 2278-2540.
- Wosu, C.O. (2024). Design of CSTR to produce 2,000,000 tons per year of magnesium chloride from neutralization of magnesium oxide and hydrochloric acid. *International Journal of Scientific and Research Publications*. 14(6), 528-548. <https://doi.org/10.29322/IJSRP.14.06.2024.p15046>.
- Wosu, C.O. & Ezech, E.M. (2024). Development of the kinetic parameters for enhanced production of ethylene glycol in a continuous stirred tank reactor. *Caritas Journal of Chemical Engineering and Industrial Biotechnology*. 1(1),
- Wosu, C. O., Ezech, E.M. & Ojong, E.O. (2024b). Development and assessment of manual and automated PID controllers for the optimum production of ethylene glycol in a CSTR. *Nigerian Journal of Tropical Engineering*. 18(2), 223-243. <https://doi.org/10.59081/njte.18.2.009>.
- Wosu, C.O., Ezech, E.M. & Owu, F.U.(2024b). Design and mechanical analysis of a continuous stirred tank reactor (CSTR) for the optimum operation and production of propylene glycol from propylene oxide hydrolysis. *Sustainable Chemical Engineering*. 5(2), 367-383. <https://doi.org/10.37256/sce.5220244713>.